Astron. Astrophys. 338, 97–105 (1998)

ASTRONOMY AND ASTROPHYSICS

Surface imaging by the Occamian approach

Basic principles, simulations, and tests

Svetlana V. Berdyugina[1,2]

[1] Astronomy Division, University of Oulu, P.O. Box 333, FIN-90571 Oulu, Finland (sveta@ukko.oulu.fi)
[2] Crimean Astrophysical Observatory, P.O. Nauchny, Crimea, 334413 Ukraine

Received 27 April 1998 / Accepted 6 July 1998

Abstract. The recently developed Occamian approach for solving inverse problems was applied to surface imaging of cool stars. With a set of tests the effects of data noise and uncertainties of the stellar parameters on the solution have been investigated. The spot locations and spot configuration are found to be well determined in most cases. The spot contrast can be successfully restored in case of adequate atmospheric models and line profile calculations. A formal error analysis of the solution is applied for the first time to the surface imaging problem. It is suggested that the pole-to-equator gradient of the temperature is a consequence of the information distribution on the stellar surface, which is determined by the available observational data. From the analysis of the error distribution on the stellar surface under different conditions two practical advices have been formulated for successful surface imaging. First, a total number points of data ought to be a few times the number of unknown parameters, since only in such a case most of the stellar surface can be restored realiably. Second, the S/N ratio should be as large as possible, since its value affects proportionally the size of the area of the stellar surface with an acceptable level of the errors.

Key words: stars: imaging – stars: activity – methods: data analysis

1. Introduction

During the last decade the surface (Doppler) imaging technique is extensively used for studying active stars. The first idea to use line profiles for mapping of the stellar surface was proposed by Deutsch (1958), while the first inversion technique with minimization was developed by Goncharsky et al. (1977). It was used for mapping chemical pecularities on the surface of Ap stars. When the periodic photometric variability of late-type active stars was interpreted as rotational modulation due to the presence of cool spots on their surface, the inverse technique was first applied to the spectra of cool stars by Vogt et al. (1987). Later contributions to the inverse technique for cool stars were by Rice et al. (1989), Collier Cameron (1990), Jankov & Foing (1992), Piskunov & Rice (1993), Kürster (1993), Unruh & Collier Cameron (1995). As an extension of the temperature and abundance mapping of the stellar surface, the magnetic (Zeeman-Doppler) imaging method was developed by Semel (1989) and Donati et al. (1989) using spectropolarimetry. The most recent review of the above contributions has been given by Rice (1996).

Different surface imaging techniques were applied to about thirty active late-type stars. It was found that the images usually show large cool features at different positions: a polar cap, high latitude spots, and low latitude spots (Strassmeier 1996). It was noticed that polar caps and high latitude spots are long-lived structures, while low latitude spots are unstable on a short time scale. Unfortunately, the validity of those features is still not established, since an error analysis is not available for the surface imaging. Also, due to different inversion methods and inputs for the line profile calculation, a comparison of the images even for a given star appears to be very difficult.

The common procedure for surface imaging is to invert the profile information to the map, using the minimization technique. However, it is known that due to noise in the data the solution with minimum deviations is too unstable and the map is very noisy. On the other hand, there are a lot of stable and smooth solutions which are compatible with the data within a given level of noise. To obtain a unique appropriate solution, some additional constraints are necessary, and at present the surface imaging techniques differ mostly by the applied constraints. The Tikhonov method (TM), which was introduced by Goncharsky et al. (1977), searches for the solution with the minimum gradient of the parameters across the map. Similarly, the maximum entropy method (MEM) used first by Vogt et al. (1987) selects the image with the minimum of information. Such kinds of smoothing are obviously artificial and in fact lead to an apparently acceptable, but distorted solution. This distortion, however, is reduced with increase of the quality of observations. On the other hand, when comparing to solar spots, one can suppose that the stellar surface with spots could be considered as having only two temperature levels. Such a strong constraint to the solution was exploited e.g. by Collier Cameron (1990) and Kürster (1993).

Recently, Terebizh & Biryukov (1994a) and Terebizh (1995a,b) elaborated a new approach to the inverse problem, which is philosophically based on the ”Occam’s razor” princi-

ple and has got the name of the 'Occamian' approach. The main advantage of the new approach is that it does not use any artificial constraints to the solution except its non-negativity, which appears quite natural for a lot of inverse problems. The resulting solution is nevertheless stable with respect to the noise in the data and uncertainties of the model calculations. Another, very important advantage of the Occamian approach is its ability to analyse the available information and use it for estimating the errors of the solution. In the present paper the Occamian approach is applied to the surface imaging problem. The stability of the solution is investigated with simulated data, and errors of the solutions are discussed.

2. The inverse problem

2.1. Basics

The surface imaging problem is related to a broad class of inverse problems, which try to determine the true properties of the phenomena from the observed effects. Thus, if we have a data set D of m points and want to restore the distribution of parameters (e.g. temperature) over the stellar surface S of n points, then the equation

$$D = PS \tag{1}$$

should be solved. Here, P denotes the Point Spread Function (PSF), or the response operator, which determines transformation of the image to the data, or the model. In the case of $n = m$, this equation could be solved in principle by simple inverting the matrix P, but the solution will be unstable due to noise in the data. Such types of problems are called ill-conditioned, or ill-posed. In more common case, $n \neq m$, the problem should be considered as a problem of parameter estimation. Then, for a given probability density function $f(D; S)$, the overall probability of obtaining the observed data is the so-called 'likelihood function'

$$L = \prod_{j=1}^{m} f(D_j; S), \tag{2}$$

given that D_j are statistically independent observations. Using the principle of maximum likelihood, one can find the solution which maximizes L and, therefore, results from the following system of the equations

$$\frac{\partial}{\partial S_i} \ln L(S) = 0, \quad i = 1, n. \tag{3}$$

Then, the solution corresponds to the highest probability to get the observed data. Note that traditionally it is $\ln L$ that is maximized, and for the Normal distribution it is the negative of the sum of squares of the residuals. Such a solution is efficient, unbiased, and has minimum variance, and, nevertheless, it is not feasible due to noise of data. There is only one way to avoid fitting the noise, namely to reduce the overall probability to some level L_0 and, therefore, fit the data reasonably:

$$L = L_0. \tag{4}$$

The level of such "reasonableness", or goodness, is determined by different tests, e.g. the chi-square test, the Kolmogorov–Smirnov test, the mean information principle, etc. Unfortunately, there are a lot of rather different solutions which satisfy the reduced level of the overall probability, and only one of them is to be chosen. It is the way of searching for this unique solution that produces different approaches to the inverse problem.

2.2. The Bayesian approach

A common way of choosing a unique solution with a given level of goodness of the fit is to invoke some additional constraints $g(S)$, which usually determine special properties of the solution, and then to maximize the functional

$$\Phi = \ln L(S) + \lambda\, g(S), \tag{5}$$

where λ is a Lagrange multiplier that should be determined under the condition of Eq. (4). Using special additional constraints on the properties of the solution, in other words *prior* information, is commonly regarded as the Bayesian approach to the inverse problem. Methods developed with such assumptions differ only with definition of $g(S)$, which sometimes is called regularization. As was mentioned, the Tikhonov method claims the solution to be with the least gradient of the parameters, and $g(S) = \mathrm{grad}S$. The maximum entropy method searches for the solution with the largest entropy, and $g(S) = S \log S$. Generally, such an approach assumes that the observed phenomena possess properties, which cannot be known *a priori*. For instance, in case of the surface imaging both above assumptions cannot be proved by the observations. In fact, for choosing a unique solution, one needs some additional information, and if it is not available, it is substituted by some plausible assumptions, which lead to an apparently acceptable solution but with a large and, in principle, unknown bias. One must note, however, that in case of data of high quality and quantity the role of the regularization is reduced, and the solution is approaching to the maximum likelihood solution, which then could be also considered as an acceptable result.

2.3. The Occamian approach

The Occamian approach was developed by Terebizh & Biryukov (1994a,1994b) and Terebizh (1995a,b) as a non-Bayesian approach to the inverse problem. In the Occamian approach the choice of the solution is based on the analysis of all available information, namely the observational data, D, and the model, P. Possessing such information, one can build a first approximation of the Fisher information matrix:

$$F(S) \approx P^T Q^{-1} P, \quad Q = \mathrm{Diag}[D_1, ..., D_m], \tag{6}$$

where the observational data D should be replaced by the model calculation R, when the solution is found, to reach the exact equality. The Fisher information matrix is known to define the error ellipsoid in the space of solutions for many inverse problems. It is ordinarily used for calculating the accuracy of the

solution. However, it can also be used for searching stable solution itself. Since $F(S)$ is a non-negative, symmetric $(n \times n)$ matrix, one can find its eigenvectors $V_1, ..., V_n$ and eigenvalues $\Lambda_1, ..., \Lambda_n$, which determine the orientation and shape of the error ellipsoid. The axes of the ellipsoid are proportional to $\Lambda^{-1/2}$. The directions of the axes define the new reference frame with the coordinates $Y_1, ..., Y_n$ which are linear combinations of the unknown parameters $S_1, ..., S_n$:

$$Y = V^T S,\ S = VY. \tag{7}$$

This orthogonal transform is the rotation of the coordinate system in the space of solutions. The new coordinates Y comprise the so-called *principal components* of the solution. Small eigenvalues of $F(S)$ indicate principal components with relatively large errors of the inverse solution, and the error ellipsoid is extremely elongated in these directions. Moreover, in case of a lack of data when $m < n$, $(n - m)$ eigenvalues become zero, and the corresponding parameters are linear dependent. Then, only a part of the principal components completely exhausts the information of S: $Y_1, ..., Y_p$, which are estimated instead of S, given the number of restrictions $S_k(Y) \geq 0,\ k = 1, ..., n$ and $Y_j = 0,\ j > p$. Then, the transform

$$\tilde{S}^{(p)} = V\tilde{Y}^{(p)} \tag{8}$$

leads to the desired stable solution $\tilde{S}^{(p)}$. The criterion for the choice of p is given by Eq. (4). Thus, the solution in the Occamian approach is that which statistically satisfactorily fits the observed data, D, with a minimum set of $\tilde{Y}^{(p)}$. Then, the solution is unique because of the choice of p and stable because of removing those principal components which contain no significant information but noise.

Note that the method has several features in common with the method of singular-value decomposition (SVD) for linear least-square problems described e.g. Press et al. (1992), especially if we represent F as $A^T A$, $A = Q^{-1/2}P$. Then, application of SVD to A gives $A = UWV^T$, $\Lambda = W^2$, and V is the same matrix as in Eq. (7). This formulation is very useful for the practical realization of the method. It allows to save the computer resources, since U is not used in the subsequent calculations. It is discussed in detail by Terebizh & Biryukov (1994a).

Thus, the solution in the Occamian approach is searched under the condition of maximum simplicity and consistency with the observational data. Apparently, English philosopher W. Occam was the first who clearly formulated the maximum simplicity requirement of a model interpreting data, in the 14th century: “Plurality is not to be assumed without necessity”. It is the well-known ”Occam’s razor” principle which could be applied to many other problems, especially in modern science. Note, that *after* the solution has been obtained, one can interpret it from the point of view of the Bayesian approach for a specially selected class of the solutions.

2.4. Present realization of the Occamian approach

For the practical realization of the method one must define the probability density function $f(D_j; S)$ and the principle for determining level L_0. The Gauss function as $f(D_j; S)$ is often used in many applications, which, however, cannot be used in case of low-signal observations. Here, the Poisson function is chosen as $f(D_j; S)$, since it approaches to the Gauss function for high signal-to-noise observations, and it is never negative for lower signals.

For testing the goodness level L_0, the mean information principle is used as was proposed by Terebizh & Biryukov (1994b). They consider that likelihood function L is to be equal to its mathematical expectation value $\langle L \rangle$ or deviates from it by a statistically insignificant value. Then, the equality $L = \langle L \rangle$ defines the class of the mean likelihood solutions. Using the Shannon definition of the information, one can find that the complete information J is $-\ln L$. Then, the mean likelihood principle is equivalent to the mean information principle, namely $J = \langle J \rangle$, and we expect to get the solution with the mean amount of information $\langle J \rangle$ rather than minimum. The value of $\langle J \rangle$ can be calculated for a given type of $f(D_j; S)$. For the Poisson function and large signals it is asymptotically about $\sum_{j=1}^{m} \ln \sqrt{2\pi e R_j}$, where R is the model calculations. For other distributions and signals this can be found in the paper by Terebizh & Biryukov (1994b). One must stress that using other principles compatible with Eq. (4) does not change the meaning of the Occamian approach.

3. The surface imaging technique

3.1. Specific properties of the problem

The technique of surface imaging was described many times by the authors mentioned above. The main idea is to trace distortions appearing in the observed line profile due to presence of spots on the stellar disk and moving due to stellar rotation. There are three important components of the problem, for which certain requirements have to be fulfilled:

Observations. High-resolution ($\lambda/\Delta\lambda \geq 30\,000$) and high signal-to-noise ratio (S/N $\geq$ 200) spectra with a good phase coverage and a few temperature sensitive spectral lines are necessary. The rotation of the star must be fast enough to use the technique (V$\sin i \geq 15$ km s^{-1}).

Input parameters. Geometrical parameters (V$\sin i$, *i*, period of rotation) and physical parameters ($T_{\rm eff}$, log *g*, microturbulence, macroturbulence) have to be known with high accuracy.

Calculation technique. Local line profile calculations and integration over the stellar surface have to be adequate for fittting observed profiles. The inversion technique chosen has to involve as few as possible assumptions.

Surface imaging is known to be a non-linear problem due to the continuum normalization of the spectra and the dependence of the line strength and shape on the local temperature. Then, the coefficients of the matrix P are functions of the parameters S. For finding a solution a few iterations are necessary, though the process converges well, if the first approximation

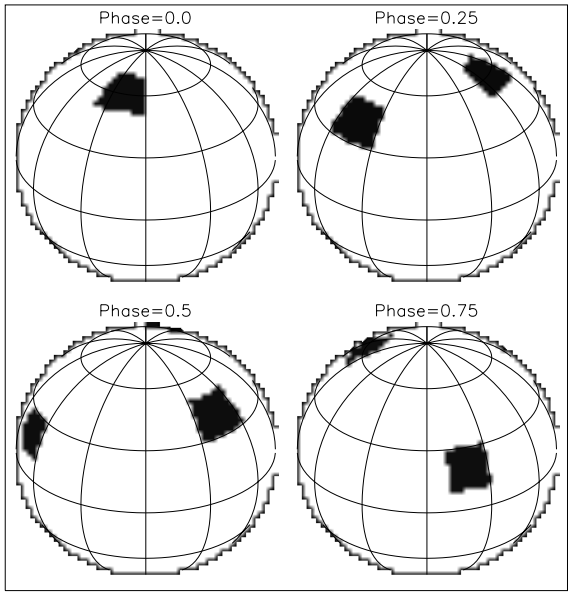

Fig. 1. The input image of the test star for the simulated data: $T_{\rm eff}$=5000 K, $T_{\rm spot}$=3500 K, log g=3.5, i=60°, Vsin$i$=50 km s^{-1}.

fits already reasonably the data. The most important parameters for choosing the first approximation are the stellar atmosphere parameters and spectroscopic line parameters, since they determine the profile which would arise in case of the unspotted star. Then, all depatures from such a profile would be interpreted as inhomogeneities on the stellar surface, and, of course, errors in those parameters will produce false features in the resulting images. An assumption on the nature of those inhomogeneities is the main part of the model calculation. For late-type active stars it was proved that it is the presence of cool spots on their surface that causes the observed periodic variability. Then, using a grid of stellar model atmospheres, one obtains the stellar image as the distribution of effective temperature across the stellar surface; this is the usual procedure in surface imaging. Obviously, the resulting temperature scale of the images is model dependent. Moreover, there are still no appropriate models for the coolest temperatures and low log g. The mentioned difficulties, however, are negligible in case of test calculations, because we use the same models for both the simulated data and the inversion procedure.

3.2. Simulations and tests

For estimating the stability of a solution one can produce a test image and compare the result of the restoration with the original image. A number of papers mentioned above have discussed effects of various uncertainties on the solution in this way. A few common intrinsic limits, which occur in stellar surface imaging, have been found with different algorithms: (1) almost total ambiguity between the hemispheres, if the inclination of the star is about 90°; (2) a lack of latitude resolution near the equator; (3) appearance of polar caps or equatorial belts due to wrong values of e.g. Vsin$i$ and i; (4) appearance of numerous false features due to errors in atomic parameters, missing blends, and phase gaps.

As a new approach to surface imaging is proposed, a set of similar tests seems to be relevant for the present paper. Though the Occamian approach provides an error analysis of the solution (see Sect. 4), a comparison of a test image with the restored one is a useful way to estimate the sensitivity of the solution to uncertainties of the input parameters. Let us assume a test star with $T_{\rm eff}$=5000 K and log g=3.5, Vsin$i$=50 km s^{-1} and i=60°. Let it have three cool spots of approximately the same projected area and $T_{\rm spot}$=3500 K. The spots are placed at different latitudes and longitudes (Fig. 1). The star is supposed to be observed in the 6415–6445 Å region, where the Fe I 6418, 6430 Å and Ca I 6439 Å lines are available, which are often used for surface imaging of cool stars. Integration over the stellar disk for producing 'observed' data has been made with high spatial resolution on the stellar surface (with a grid 1°×1°). A list of atomic line parameters was obtained from VALD (Piskunov et al. 1995) for lines having a central depth of 1% or more. A number of molecular lines was included to the list, since the presence of numerous molecular lines in the spectra of stars with effective temperature $T_{\rm eff}<$5000 K is quite noticeable. Stellar model atmospheres used are from Kurucz (1993). A code used for the synthetic-spectrum calculations is described in detail by Berdyugina (1991). It includes calculations of opacities, intensities and fluxes in the continuum and in atomic and molecular lines. Also, the number densities of atoms and molecules are calculated under the assumption of dissociative equilibrium.

For the first, 'ideal', reconstruction a moderate value of the signal-to-noise ratio (S/N=200) and twenty equally spaced phases have been simulated with resolving power 60 000. All three lines mentioned were available. The parameters of the star, e.g. Vsin$i$, i, $T_{\rm eff}$, and log g are supposed to be known precisely. For the inversion a grid of 6°×6° on the stellar surface has been used. With the adopted inclination, it consisted of n=1500 pixels. The result of the reconstruction is shown in Fig. 2. One can see that the position of the spots, their projected area and contrast are well determined, and there are no false features of noticeable contrast. The fit to the data corresponds to the adopted value of S/N. The temperature scale is well restored, too.

In practice, often only poor observations are available, and many parameters are not known exactly. For that reason, a set of tests has been carried out for studying effects of various uncertainties. The input parameters for the tests are presented in Table 1 (Test 1–8), and some comments to the solutions are briefly reported. The resulting images for the tests are shown in Fig. 3. One can notice that some intrinsic limits of the problem mentioned are found with the new approach, as was expected. However, one can conclude that the spot locations (and spot configuration) are well determined in most cases, and they are the most reliable result, even in the case of S/N=100. False features appearing due to some wrong parameters are of lower contrast in comparison to real spots, and there is no problem to distinguish them in these test cases. The spot contrast is well determined in case of adequate atmospheric models and line profile calculations. However, since the difference between the

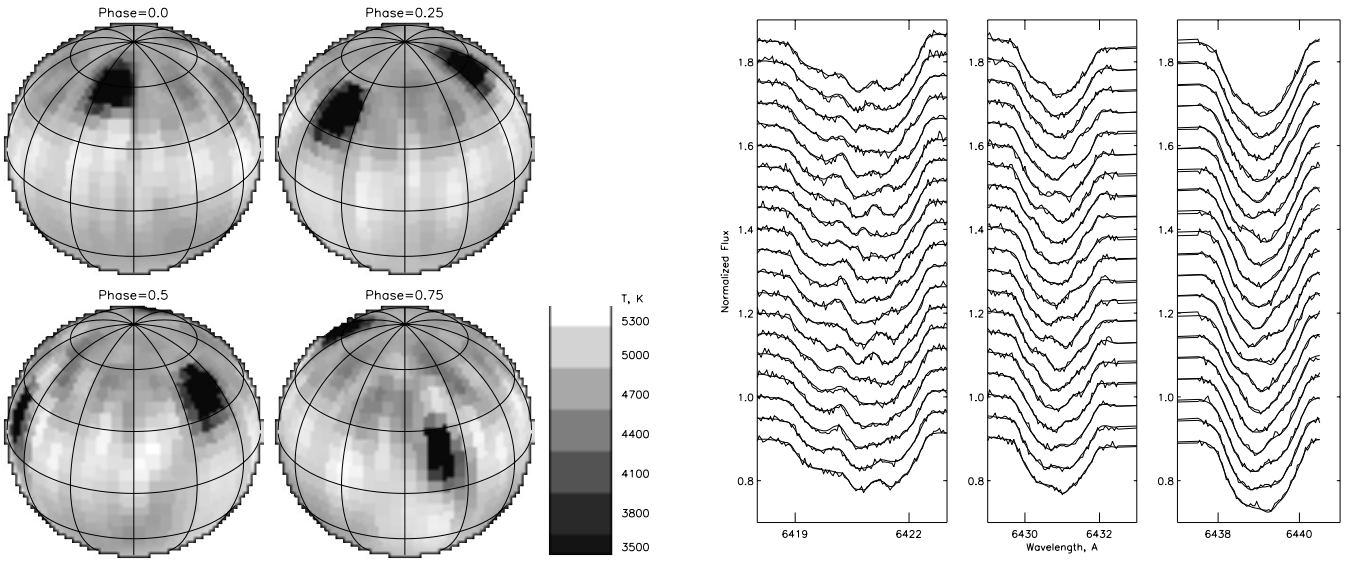

Fig. 2. The restored image of the test star from the simulated data under good condition (left): S/N=200, 20 equally spaced phases, Fe I and Ca I lines in the 6415–6445 Å region, all parameters of the star are known precisely. A fit to the simulated data is shown in the right panels: 'observed' data are shown by thin lines, while thick lines represent the calculated line profiles based on the reconstructed image. Profiles of consecutive phases have been shifted in the vertical direction. Phase is increasing from bottom to top.

Table 1. Effects of various parameter uncertainties and spot locations. The parameters which are not mentioned are assumed to be known precisely.

Test	Parameters	Comments
	A lack of observations and the effect of low S/N	
1	1 line Ca I, 20 phases, S/N=200	the restored image is blurred,
	n=1500, m=1220, p=355	spot positions are well determined
2	S/N=100, 3 lines, 20 phases	image is more noisy and blurred,
	n=1500, m=4780, p=1394	sports are still at the correct positions
	Effect of wrong Vsini	
3	Vsin$i$=48 km s^{-1}, S/N=200, 20 phases, 3 lines	dark polar cap and bright equatorial
	n=1500, m=4780, p=1383	belt of moderate contrast
4	Vsin$i$=52 km s^{-1}, S/N=200, 20 phases, 3 lines	bright polar cap and dark equatorial
	n=1500, m=4780, p=1383	belt of moderate contrast
	Effect of wrong inclination	
5	i=50°, S/N=200, 20 phases, 3 lines	higher spot latitudes
	n=1500, m=4780, p=1267	
6	i=70°, S/N=200, 20 phases, 3 lines	lower spot latitudes
	n=1620, m=4780, p=1515	
	Effect of wrong $T_{\rm eff}$	
7	$T_{\rm eff}$=4900K, 1 line Ca I, S/N=200, 20 phases	dark polar cap
	n=1500, m=1220, p=355	
8	$T_{\rm eff}$=5100K, 1 line Ca I, S/N=200, 20 phases,	reduced spot contrast in higher latitudes
	n=1500, m=1220, p=355	
	Equatorial spots	
9	S/N=200, 20 phases, 3 lines,	reduced spot area and contrast,
	n=1500, m=4780, p=1375	sub-equatoral spots are not restored

real atmosphere and its model is unknown, especially regarding spot models, the spot contrast restored from real observations can be wrong and should be checked with e.g. photometric observations.

From the test calculations a pole-to-equator gradient of the temperature distribution is often seen on the stellar surface, especially for wrong values of Vsin$i$ and $T_{\rm eff}$. These parameters affect significantly the spectral line depths, which are corrected in the inversion by introducing the temperature gradient over the stellar surface. The pole-to-equator gradient of the temperature (or brightness) distribution was also noticed with other methods (see e.g. review by Rice 1996). The most known example of this gradient is a cool polar cap restored on many late-type stars. As is seen from Tests 7 and 8, the errors in $T_{\rm eff}$ of $\pm$100K

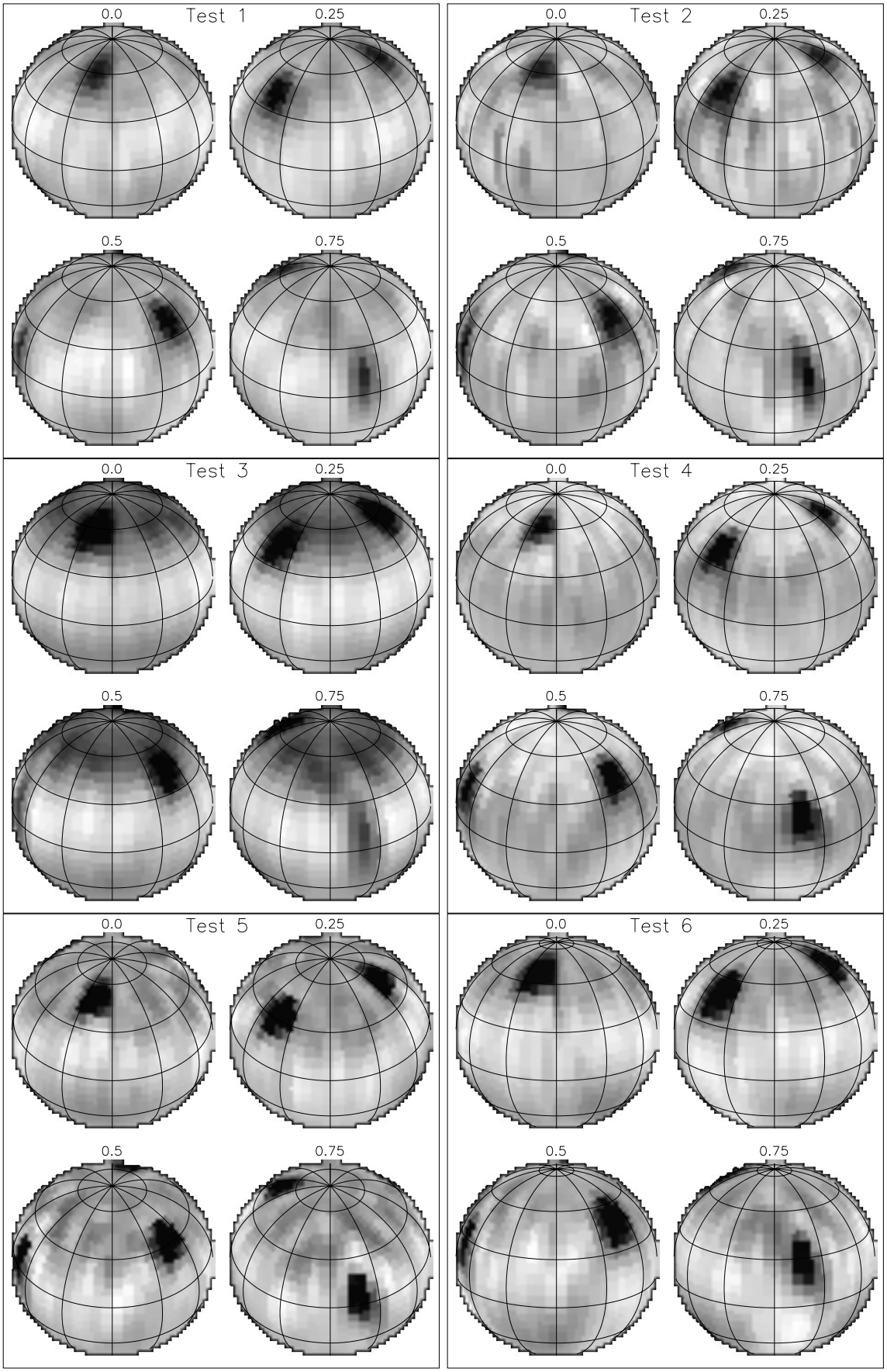

Fig. 3. Restored images of the test star from the simulated data (see comments in Table 1).

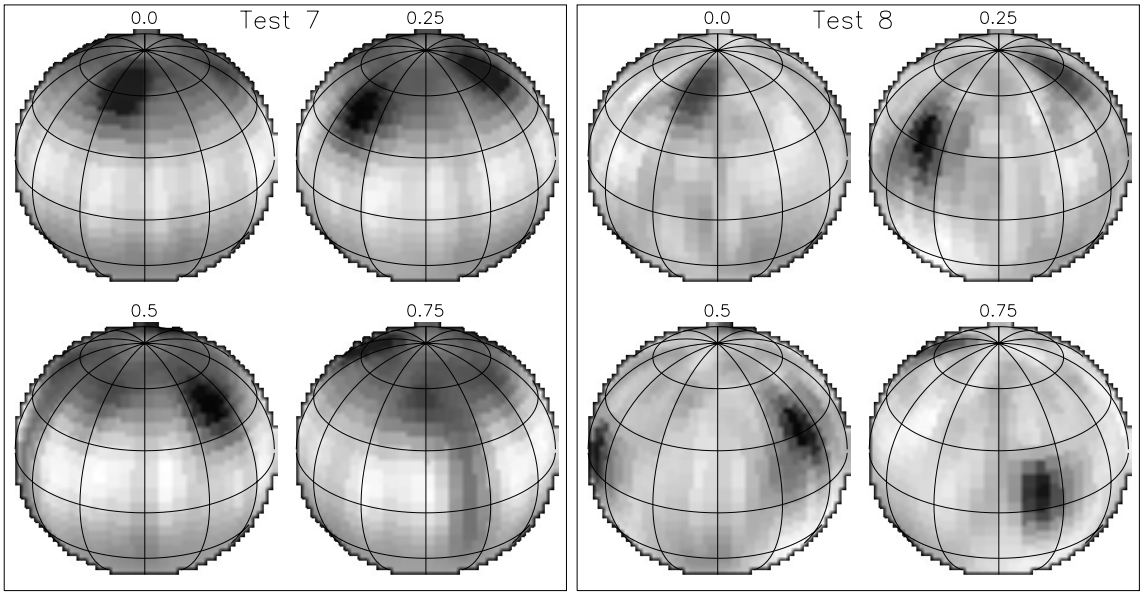

Fig. 3. (continued)

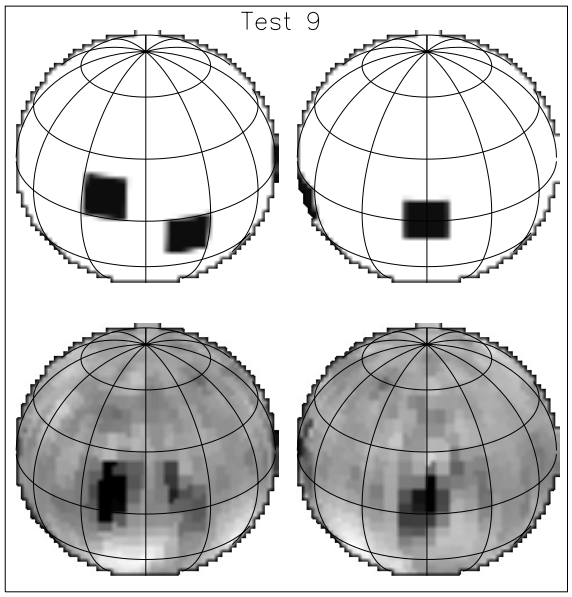

Fig. 4. Images of the test star with equatorial spots: input images are in the top, and images restored from the simulated data are in the bottom (see comments in Table 1 for Test 9).

can noticeably affect the solution obtained with a limited set of line profiles, though in practice $T_{\rm eff}$ is often known with larger errors. Significant underestimation of $T_{\rm eff}$ can result in a much more contrast polar cap, which will be then a dominative feature of the map. As is shown in Sect. 4, the temperature gradient is a consequence of the information distribution on the stellar surface, which is determined by the available observational data.

The lowest latitude spot in Tests 1–8 is found to be very sensitive to the uncertaities of the parameters. Its contrast and area are changing drastically for different cases, though the position is often well determined. As was mentioned, the problem of surface imaging shows the effect of a lack of latitude resolution near the equator. Therefore, one more test has been calculated with the input image consisted of equatorial and near equatorial spots (Test 9, Fig. 4). It is seen from the test that sub-equatorial parts of the spots are not restored and, possibly, partly reflected to the over-equatorial latitudes. Thus, the probability a spot to be restored is a strong function of latitude, and it is in a good agreement with the error distributions estimated in Sect. 4.

4. Error analysis

4.1. Basics

If n is the number of unknown parameters, we can determine the $n \times n$ variance matrix of the solution $\tilde{S}$:

$$\Omega(S) = (\tilde{S} - S) \times (\tilde{S} - S)^T, \tag{9}$$

where S is the true object, namely the vector of true values of the unknown parameters. Generally, to solve the problem means to find such a solution $\tilde{S}$ which results in small values of the diagonal elements of the matrix $\Omega(S)$. Non-diagonal elements of it reflect the degree of linear dependence of the parameters. Since S is always unknown, the variance matrix cannot be found. However, knowing the Fisher matrix, which is used by the Occamian approach, helps to estimate the lower limit of $\Omega(S)$. The following inequality is justified:

$$\Omega(S) \geq F^{-1}. \tag{10}$$

Thus, the variances of the solution, which are the diagonal elements of $\Omega(S)$, can be estimated as

$$\sigma^2(\tilde{S}) \geq \mathrm{Diag}[F^{-1}]. \tag{11}$$

More details on the validity of such an estimate can be found in the reviews by Terebizh (1995a,b). Note that the equality in

Eqs. (10) and (11) is achieved only for a certain type of probability density functions and for unbiased solutions. However, even in case when the equality is impossible, the solution $\tilde{S}$ can be close enough to the estimate which is determined by those equations.

Thus, at present, for the first time in surface imaging, one can study the formal errors of the solution rather than discuss visible coincidence of the input and output images.

4.2. Error analysis for the test calculations

The inverted Fisher matrix has been calculated for all tests. The error distribution, $\sigma(\tilde{S})$, is found to be a strong function of latitude. Such a distribution appears to determine the known sensitivity of the surface imaging problem to the latitude extension of the restored features. The most interesting results, for the 'ideal' restoration and Tests 1 and 2, are presented in Fig. 5.

Most of the stellar surface in Test 1 is formally underdetermined due to the lack of the available data: one spectral line, $n < m$, and $p \ll n$. Then, a substantial part of the restored parameters are linearly dependent, and, therefore, they and their errors are formally not defined. However, if most of the linear dependent parameters are successfully *guessed*, as in Test 1 where $T_{\rm eff}$ is known precisely, the solution is close enough to the real object. Thus, the errors in correspondent parts of the stellar surface are determined mostly by the uncertainty of $T_{\rm eff}$ (as in Tests 7 and 8). In other words, the number of the linear dependent parameters denotes the stability of the solution to the uncertainty of $T_{\rm eff}$. One must stress that using only one spectral line for surface imaging with high spatial resolution on the stellar surface appears to be the common approach. However, as is seen from the error distribution, such a practice can result in large uncertainties in most of the resulting image, especially in cases when not all input parameters are known precisely, which commonly happens with real observations. Then, even averaging of images obtained from particular lines cannot significantly improve the result. The averaging is formally reducing errors, but it cannot substitute missing information and solve the underdetermined problem. Taking into account this effect, one can easily explain visible fast variability of low-latitude features, which has been restored on the surfaces of many cool active stars.

As in Test 1, the underdetermined parts are seen in the 'ideal' restoration and Test 2 for latitudes less than -30°, where the projection of the stellar elementary areas is close to zero, and the observed profiles do not contain significant information of those parts. One can see that the errors are quite large, usually about 100-300K for over-equatorial latitudes and more for lower latitudes in the best case of the 'ideal' restoration. However, one should note again, that these formal estimates are obtained without incorporation any information on $T_{\rm eff}$, though it is used for the first approximation of the solution, or unspotted stellar surface. If $T_{\rm eff}$ is not known (or known with some error), the *formal* error estimates will be the same as before, but the real errors are much larger. The accuracy of the solution is determined by the *real* amount of the information on the temperature contained in the limited set of line profiles.

For the 'ideal' restoration (S/N=200) the area with a satisfactory level of the errors ($\sigma \leq$300K) extends in latitudes for about 75° around the pole, while for Test 2 (S/N=100) the errors increase up to 400K within the same latitudes. For Test 1 the area available for analysis is only 30° around the pole while the smallest errors are crowded next to the very pole. For Tests 3–6 the error distributions are similar to the 'ideal' restoration because of the similar values of n, m, p and the S/N ratio. There is an obvious tendency for the errors to increase towards lower latitudes, which can be understood from the point of view of the visibility of the stellar surface for the observer: the pole region is seen in all rotational phases, while others are observable only at certain phases. Such distribution of the errors can result in the qualitatively similar temperature distribution on the stellar surface, especially when the temperature of the unspotted surface is known with a large error. Then, the pole-to-equator gradient of the temperature distribution noticed in the stellar images is determined by the properties of the problem, namely by the distribution of the available information over the stellar surface.

From the analysis of the error distribution under different conditions one can formulate practical advices for successful surface imaging. First, the total number of data points, m, ought to be a few times the number of unknown parameters, n. It means that all components of m, namely spectral resolution and number of profiles and phases, have to be increased as much as possible. Only in such a case the number of principal components of the solution, which contain significant information on the restored image, p, will be close enough to n, and most of the stellar surface can be restored realiably. Increasing the stellar image resolution (namely, increasing n) is impossible without a sufficient *quantity* of observations. Typical values of n and m, which can be found in papers on surface imaging, are about $\geq$2000 and $\leq$1000, respectively, though everyone knows that it is impossible to find two parameters with one measurement. Second, the *quality* of the observations, here the S/N ratio, also affects the size of the area of the stellar surface with an acceptable level of the variances. As is seen in Fig. 5, twice the S/N ratio is proportionally reducing the errors. Thus, the value of S/N should be as large as possible. The latter was also concluded by other athours, though it was proved only with simulations.

Note that in the case of the above simulations, it would be possible to calculate also the variance matrix $\Omega(S)$ with Eq. (9), since we know the true object, the input image. It has been done, and it was found that the errors for Tests 1–8 are within 100K–400K, and the errors in the sub-equatorial latitudes are determined by the adopted temperature for the first iteration, since no spots are assumed to be present in those latitudes. For Test 9 the errors in equatorial and sub-equatorial parts are quite large, namely up to 1000K, since the spots are only partly restored.

5. Summary

The recently developed Occamian approach for solving inverse problems was applied to surface imaging of cool stars. Two main advantages of the new approach differ it significantly from the approaches which were used previously in surface imaging:

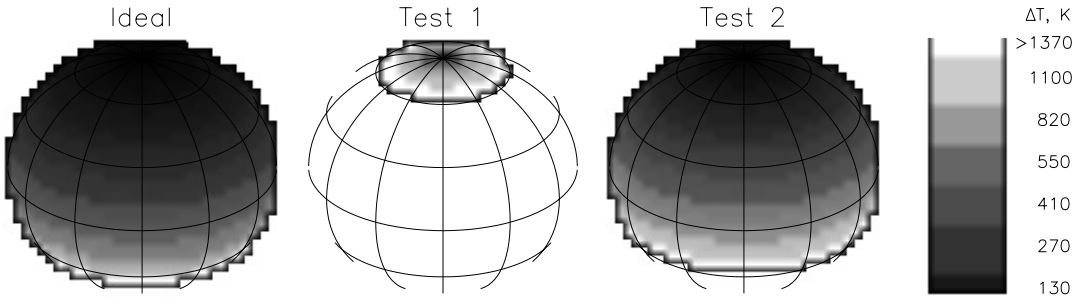

Fig. 5. Error distribution on the stellar surface for the 'ideal' restoration of the test star image and Tests 1 and 2. Most of the stellar surface in Test 1 is underdetermined due to the lack of available data (one spectral line, $m < n$) and, therefore, a linear dependence of most parameters. The same situation is seen for the 'ideal' restoration and Test 2 for latitudes less than –30°. For the 'ideal' restoration (S/N=200) an area with a satisfactory level of the errors ($\sigma \leq 300\ K$) extends for 75° around the pole, while for Test 2 (S/N=100) one obtains only 40°. For Test 1 the area available for analysis is only 30° around the pole, and the smallest errors are crowded next to the very pole.

1. It does not use any artificial constraints to the solution except its non-negativity, but the resulting solution is nevertheless stable with respect to the noise in the data and uncertainties of the model calculations.

2. It is able to analyse the available information and use it for estimating the errors of the solution.

With a set of tests the effects of data noise and uncertainties of the stellar parameters on the solution have been investigated. It was found that the spot locations and spot configuration are well determined in most cases, and they are the most reliable result. False features appearing due to some wrong parameters are less contrast in comparison to the real spots. The spot contrast is well determined in case of adequate atmospheric models and line profile calculations.

A formal error analysis of the solution is applied for the first time to the surface imaging problem. It is suggested that the pole-to-equator gradient of the temperature is a consequence of the information distribution on the stellar surface. The latter is determined by the available observational data. It is shown that a lack of data can result in most of the stellar image to be underdetermined, especially in the lower latitudes. Then, visible fast variability of low latitude features, which has been restored on the surfaces of many cool active stars, seems to be caused by the non-stability of the solutions.

From the analysis of the error distribution on the stellar surface under different conditions two practical advices have been formulated for successful surface imaging. First, a total number points of data ought to be a few times the number of unknown parameters, since only in such a case most of the stellar surface can be restored realiably. Second, the S/N ratio should be as large as possible, since its value affects proportionally the size of the area of the stellar surface with an acceptable level of the errors.

Acknowledgements. I am very grateful to the authors of the Occamian approach Dr. V.Yu. Terebizh and V.V. Biryukov for consultations and useful practical advices for the successful realization of the method. I am thankful also to Dr. R.E. Gershberg for encouraging this work and Dr. J.B. Rice, Dr. K.G. Strassmeier and Prof. I. Tuominen for the interest to apply the method to real observations. Dr. R. Duemmler is thanked for his useful discussion of the paper. I thank also the referee, Dr. A. Collier Cameron, for useful suggestions which helped to improve the paper.

References

Berdyugina S.V., 1991, Izv. Krymsk. Astrofiz. Obs. 83, 102
Collier Cameron A., 1990, in Surface Inhomogeneities on Late-Type Stars, Lecture Notes in Physics 397, P.Byrne and D.Mullan (eds.), Springer-Verlag, p. 33
Deutsch A., 1958, in Electromagnetic Phenomena in Cosmical Physics, IAU Symp. 6, B.Lehnert (ed.), Cambridge University Press, p. 209
Donati J.-F., Semel M., Praderie F., 1989, A&A 225, 467
Goncharsky A.V., Stepanov V.V., Khokhlova V.L., Yagola A.G., 1977, Sov. Astron. Letters 3, 147
Jankov S., Foing B., 1992, A&A 256, 533
Kurucz R.L., 1993, Kurucz CD No. 13
Kürster M., 1993, A&A 274, 851
Piskunov N.E., Rice J., 1993, PASP 105, 1415
Piskunov N.E., Kupka F., Ryabchikova T.A., Weiss W.W., Jeffrey C.S., 1995, A&AS 112, 525
Press W.H., Teukolsky S.A., Vetterling W.T., Flannery B.P., 1992, Numerical Recipes, Cambridge Univ. Press, Cambridge
Rice J.B., 1996, in IAU Symposium 176, Stellar Surface Structure, K.G.Strassmeier, J.L.Linsky (eds.), Kluwer Academic Publishers, p. 19
Rice J.B., Wehlau W.H., Khokhlova V.L., 1989, A&A 208, 179
Semel M., 1989, A&A 225, 456
Strassmeier K.G., 1996, in IAU Symposium 176, Stellar Surface Structure, K.G.Strassmeier, J.L.Linsky (eds.), Kluwer Academic Publishers, p. 289
Vogt S.S., Penrod G.D., Hatzes A.P., 1987, ApJ 321,496
Terebizh V.Yu., 1995a, Physics–Uspekhi 38, 137 (translated from Uspekhi Fiz. Nauk 165, 143)
Terebizh V.Yu., 1995b, Int. J. Imaging Systems and Techn. 6, 358
Terebizh V.Yu., Biryukov V.V., 1994a, A&SS 218, 65
Terebizh V.Yu., Biryukov V.V., 1994b, Astron.&Astrophys. Trans. 6, 37
Unruh Y.C., Collier Cameron A., 1995, MNRAS 273, 1